

Article

Effect of Humic Acid Binder on Oxidation Roasting of Vanadium–Titanium Magnetite Pellets via Straight-Grate Process

Yihui Yi ^{1,2}, Guanghui Li ^{1,2} , Pengxu Cao ^{1,2}, Xin Zhang ^{1,2,*} , Yongkang Zhang ^{1,2}, Jin Zhang ^{1,2} and Jiahao Huang ^{1,2}

¹ School of Minerals Processing and Bioengineering, Central South University, Changsha 410083, China; 155601011@csu.edu.cn (Y.Y.); liguangh@csu.edu.cn (G.L.); caopengx@csu.edu.cn (P.C.); 185601018@csu.edu.cn (Y.Z.); zhangjinsx@csu.edu.cn (J.Z.); 205611059@csu.edu.cn (J.H.)

² National Engineering Laboratory for High Efficiency Recovery of Refractory Nonferrous Metals, Changsha 410083, China

* Correspondence: zhangxinnv@csu.edu.cn; Tel.: +86-731-88830542

Abstract: The oxidation roasting of vanadium–titanium magnetite (VTM) pellets with a new composite binder was investigated using a pilot-scale straight-grate. The evolution of the chemical and phase composition, the compressive strength, and the metallurgical properties of the fired VTM pellets were investigated. Under a preheating temperature of 950 °C, a preheating time of 18 min, a firing temperature of 1300 °C, and a firing time of 10 min, the compressive strength of the fired pellets was as high as 2344 N per pellet. The fired pellets mainly consisted of hematite, pseudobrookite, spinel and olivine. The total iron content of the fired pellets was 0.97% higher using 0.75 wt% humic acid (HA) binder instead of 1.5 wt% bentonite binder. These properties are beneficial for the production efficiency and energy efficiency of their subsequent use in blast furnaces. Moreover, both the softening interval and the softening melting interval of the HA binder pellets were narrower than those of the bentonite binder pellets, conducive to the smooth and successful smelting of the VTM pellets in a blast furnace.

Keywords: humic acid binder; oxidation roasting; vanadium-titanium magnetite pellets; straight-grate process



Citation: Yi, Y.; Li, G.; Cao, P.; Zhang, X.; Zhang, Y.; Zhang, J.; Huang, J. Effect of Humic Acid Binder on Oxidation Roasting of Vanadium–Titanium Magnetite Pellets via Straight-Grate Process. *Crystals* **2021**, *11*, 1283. <https://doi.org/10.3390/cryst11111283>

Academic Editors: Yufeng Guo, Shuai Wang, Mao Chen, Kexin Jiao, Lingzhi Yang, Feng Chen and Fuqiang Zheng

Received: 20 September 2021
Accepted: 12 October 2021
Published: 22 October 2021

Publisher's Note: MDPI stays neutral with regard to jurisdictional claims in published maps and institutional affiliations.



Copyright: © 2021 by the authors. Licensee MDPI, Basel, Switzerland. This article is an open access article distributed under the terms and conditions of the Creative Commons Attribution (CC BY) license (<https://creativecommons.org/licenses/by/4.0/>).

1. Introduction

Pelletizing is one of the most important agglomeration processes for producing high-quality, structurally sound, and metallurgically sound feed for blast furnaces and direct reduction [1]. The binder used in pelletizing processes has a significant effect on the preparation and overall quality of the resulting pellets. Sodium bentonite, which mainly consists of aluminum and silicon minerals with high moisture adsorption capacities, is the most common binder for iron ore pellets [2,3]. Sodium bentonite is usually added in an amount of 1.5–3.0 wt% by weight of the iron concentrate in China, which is much higher than the average level of 0.6–0.8 wt% in the rest of the world [4,5]. The presence of bentonite causes some aluminum and silicon impurities to enter the resulting pellets, which significantly reduces their iron grade and increases the energy consumption and cost of iron-making [6]. Organic binders, which have the advantages of lower dosage, almost no residue production, and enhanced pellet strength, are promising substitutes for bentonite [7]. The most prominent organic binders include Peridur, carboxymethylcellulose (CMC)-based binders, polyacrylamide-based binders, and various types of modified starch [8,9]. However, organic binders have not been widely used in China because the compression strength of the resulting preheated and fired pellets is insufficient and does not meet the requirements of grate-kiln processes.

An innovative binder extracted from lignite and based on humic acid (HA) has been invented by our research group [10,11]. This binder has the advantages of high bonding

ability and low residue generation, and the thermostability of this composite binder is superior to that of pure organic binders. Pellet production by direct reduction has been achieved using this composite humic acid-based binder. However, it has not yet been used in the industrial production of oxidized pellets.

Both straight-grate and grate-kiln furnaces are widely used in oxidized pellet production [12]. Grate-kiln furnaces consist of three separate machines linked in series. Pellets are preheated in a traveling grate then physically transferred to a rotating kiln for firing. Straight-grate furnaces require slightly less capital expenditure to build compared to grate-kiln furnaces because they do not require as much vertical framework [13]. Moreover, pellets in straight-grate furnaces are mostly immobile, meaning that the required compression strength of preheated pellets in straight-grate processes is lower than that in grate-kiln processes. Hence, straight-grate processes are more suitable for organic binders and humic acid-based binders.

Vanadium–titanium magnetite (VTM) is an important source of V, Ti, and Fe, of which China has a reserve of more than 30 billion tons [14,15]. The major challenge of the industrial manufacturing of VTM oxidized pellets is the high bentonite dosage. This study is a first attempt to apply a humic acid binder in oxidation roasting of vanadium–titanium magnetite (VTM) pellets, specifically via the straight-grate process, with the aim of exploring the optimal operating conditions for the drying, preheating, and firing of the pellets. The physical and chemical properties of the fired vanadium–titanium magnetite pellets during the straight-grate oxidization process were investigated based on the pilot-scale operating conditions.

2. Materials and Methods

2.1. Materials

The vanadium–titanium magnetite concentrates and bentonite used in this study were obtained from Sichuan Province, China, and their chemical compositions are listed in Table 1.

Table 1. Chemical composition of VTM concentrate and bentonite/wt%.

Component	TFe	FeO	SiO ₂	Al ₂ O ₃	CaO	MgO	TiO ₂	V ₂ O ₅	K ₂ O	Na ₂ O
VTM	55.45	32.36	4.39	3.05	0.75	3.16	11.17	0.61	0.02	0.11
Bentonite	-	-	59.66	12.43	4.60	3.40	-	-	0.94	2.68

Table 1 shows that the total iron (TFe) content of the VTM concentrate was 55.45 wt% and its TiO₂ content was 11.17 wt%, mostly due to its titanomagnetite phase. Bentonite, comprised of 59.66 wt% SiO₂ and 12.43 wt% Al₂O₃, was used as the inorganic binder for this study. The VTM concentrate had a particle size of less than 0.074 mm, a mass fraction of 88.92%, and a specific surface area of 1944 cm²·g⁻¹.

The humic acid-based binder used in this study was extracted from lignite in Guizhou Province, China. The industrial analysis results and the chemical composition of the binder ash are shown in Table 2. The ash content of the HA binder was 39.51 wt%, indicating that the fired pellets will have fewer residues. The main components of the HA binder ash were SiO₂, Al₂O₃, and Na₂O, which represent 56.90 wt%, 24.69 wt%, and 6.80 wt% of the binder ash, respectively.

Table 2. Industrial analysis of humic acid-based binder and the chemical composition of the binder ash/wt%.

Component	Mad	Aad	Vad	FCad	Ash Chemical Composition/wt%					
					TFe	SiO ₂	Al ₂ O ₂	CaO	K ₂ O	Na ₂ O
Content	15.62	39.51	18.21	26.66	2.52	56.90	24.69	0.58	2.48	6.80

Mad: the moisture; Aad: the ash; Vad: the volatiles; FCad: the fixed carbon.

Compared to inorganic binders, organic binders undergo combustion at higher temperatures, which is problematic for obtaining strong pellets. Meanwhile, the void space left behind as organic binders combust is typically well-connected, allowing for good inflow of reducing gases [16]. The thermogravimetric and differential scanning calorimetry (TG-DSC, STA449 F5, NETZSCH, Selb, Germany) curves of the HA binder are shown in Figure 1. The HA binder DTG curve showed three distinct mass loss peaks during the roasting process, with a total HA binder mass loss of 58.64%. Correspondingly, two endothermic peaks and one exothermic peak appeared in the DSC curve. First, an endothermic peak appeared at 93.5 °C due to the dehydration of the HA binder's crystallized water, representing a mass loss of 10.48%. When the temperature was increased from 200 °C to 700 °C, a rapid mass loss of 42.12% occurred, as shown by the significantly exothermic peaks. This was due to the decomposition and depolymerization of the organic structure as well as the combustion of carbon. Furthermore, a mass loss peak at 1092.4 °C, representing a mass loss of 4.94%, was attributed to condensation polymerization.

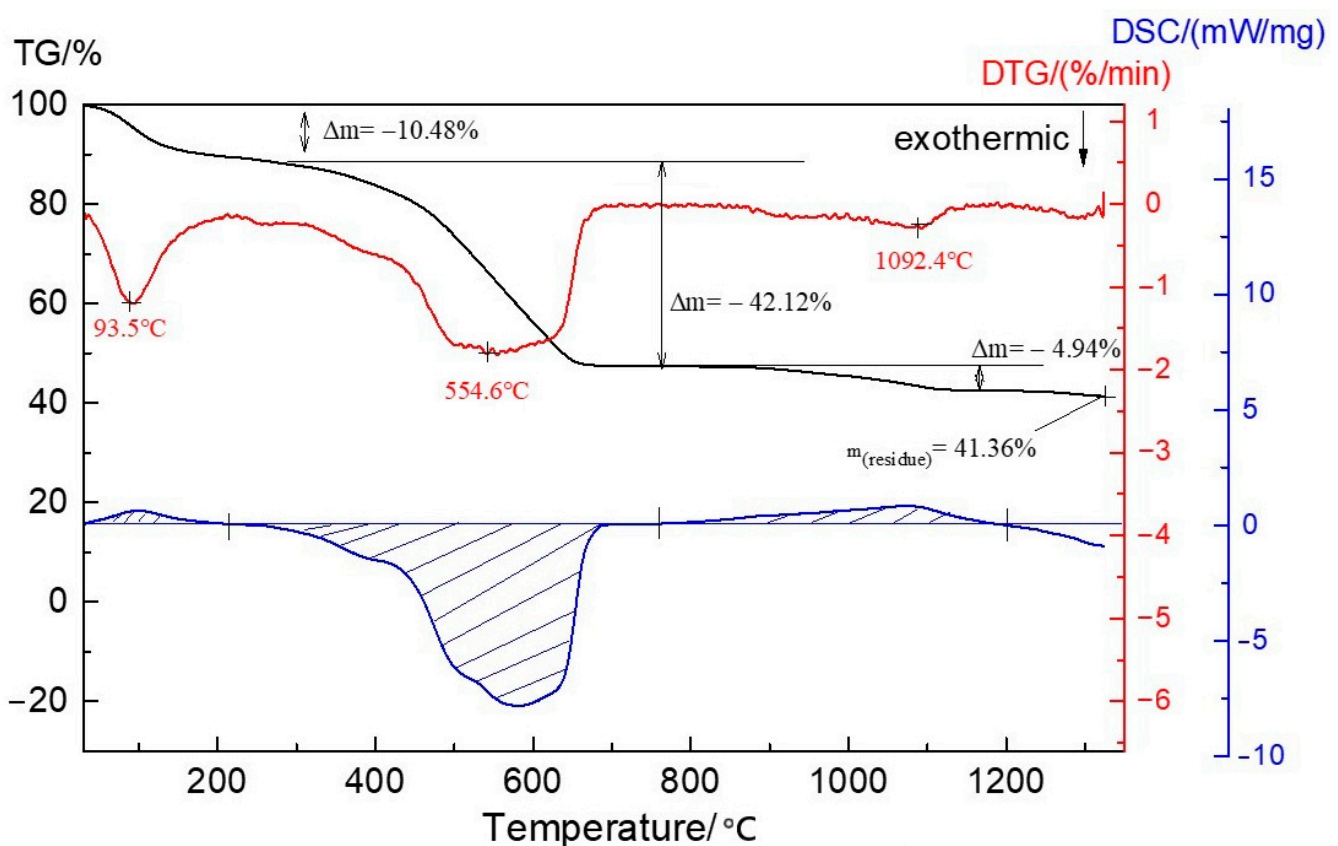


Figure 1. TG-DSC curves of HA binder (air atmosphere, 10 °C/min).

The organic structure of the HA binder affects the interfacial interaction between the binder and the VTM particles. Figure 2 shows the Fourier-transform infrared (FTIR) spectra of the HA binder. The peak at 3418.84 cm^{-1} was attributed to the stretching vibration of $-\text{OH}$ associated with hydrogen bonding and the peak at 1575.31 cm^{-1} was attributed to the vibration of $\text{C}=\text{C}$ bonds in aromatic rings. The stretching vibrations of $-\text{OH}_{\text{ph}}$ or $\text{C}-\text{H}$ in aliphatic hydrocarbons resulted in a peak at 1385.63 cm^{-1} . Furthermore, the peak at 1032.66 cm^{-1} was attributed to the stretching vibration of $\text{Si}-\text{O}$ and the peaks at 798.41 cm^{-1} , 777.17 cm^{-1} , and 694.25 cm^{-1} belonged to the out-of-plane swing bending of $\text{C}-\text{H}$ in aromatic rings. The peaks at 537.07 cm^{-1} and 473.44 cm^{-1} were attributed to the stretching vibration of $\text{C}-\text{S}$ and $\text{S}-\text{S}$, respectively. Based on these results, it was determined that the organic compounds in the HA binder were mainly carboxyl groups, hydroxyl groups, aromatic rings, and aliphatic hydrocarbons.

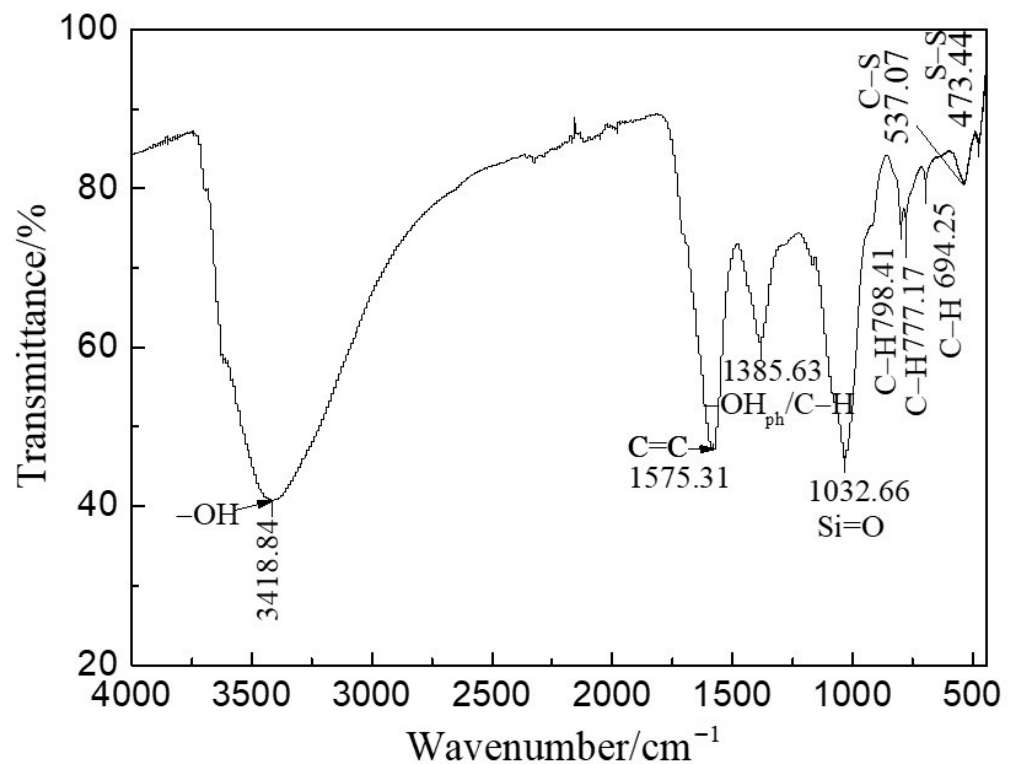


Figure 2. FTIR spectrum of HA binder.

HA molecules were mainly adsorbed onto VTM particles via ligand exchange and complexation, while bentonite was mainly adsorbed through physical adsorption. Metallic cations that dissolve from the surface of the VTM particles played a bridge role in the adsorption of the HA binder onto the VTM particles [17]. The main functional groups involved in the complexation of the HA binder are shown in Figure 3. These functional groups include carboxyl groups, phenolic hydroxyl groups, C=C groups, and $-NH_2$ groups.

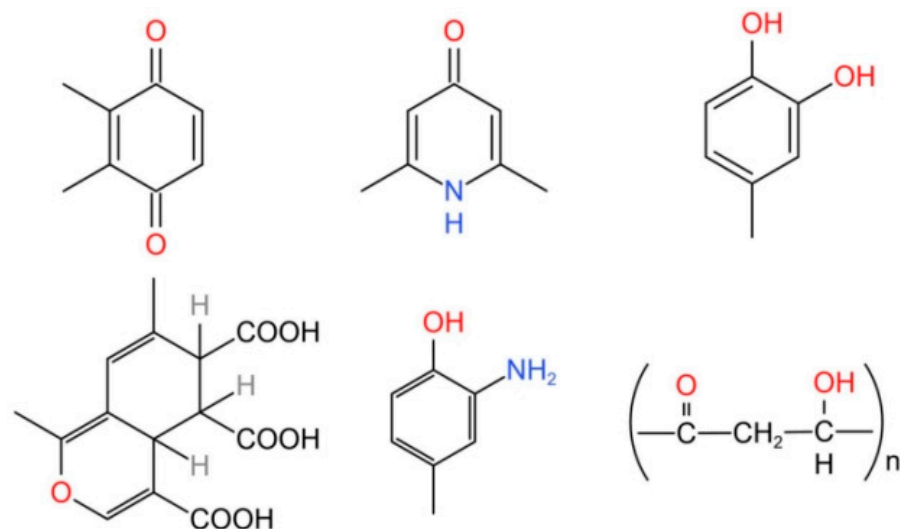


Figure 3. The main functional groups involved in the complexation of the HA binder.

2.2. Methods

2.2.1. Balling Process

The initial moisture content of the VTM concentrates was adjusted to 7.0 wt%. For each pilot-scale experiment, 30 kg VTM concentrate was thoroughly mixed with a set amount of bentonite (1.50 wt%) or HA binder (0.75 wt%). The binder amounts were optimized through

evaluating the compressive strength and drop strength of the green pellets, as shown in Figure 4. The green pellets with drop strength higher than three times when dropped from 0.5 m and a compressive strength higher than 10 N per pellet were used for the subsequent experiment (the reported drop strength and compressive strength figures are the average of 10 pellet tests) [1].

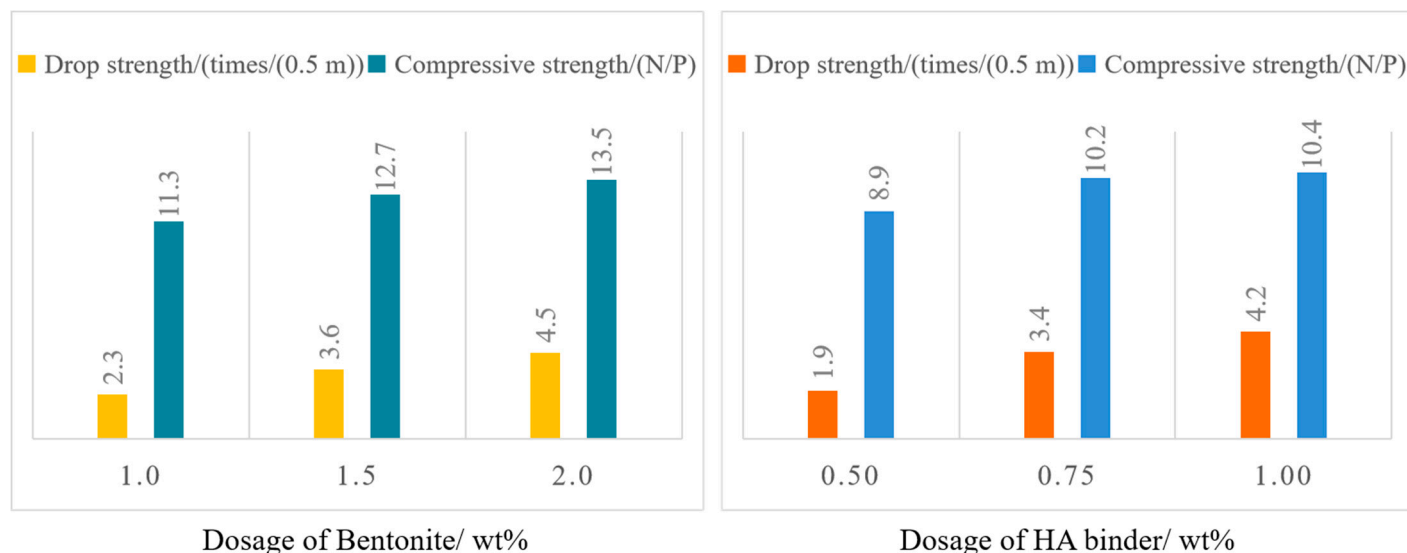


Figure 4. Effect of binder amounts on the qualities of VTM green pellets.

After mixing, the mixtures were pelletized for 20 min by a disc pelletizer (diameter 1 m, inclination angle 45°, rotational speed 23 rpm). A portion of the resulting green pellets with diameters of 10–16 mm was selected to investigate the compression strength, drop strength, and shock temperature of the pellets. The same green pellet diameter range was used for the subsequent oxidation roasting process.

2.2.2. Oxidation Roasting Process

A traveling grate was used to simulate a straight-grate facility. This grate consisted of a chain cup, an air mixed chamber, a vacuum chamber, and sealing and discharging units, as shown in Figure 5. The inside diameter and the height of the chain cup were 280 mm and 450 mm, respectively. The qualified green pellets were fed into the chain cup for the pilot-scale experiment, and a layer of fired pellets beneath the green pellets was used to protect the steel grate cars from extreme furnace temperatures. The height of the green pellets was 300 mm and the height of the hearth layer was 100 mm.

The drying process included one updraft drying stage and two downdraft drying stages. During updraft drying, valves #3 and #4 were opened, while valves #2 and #5 were closed. These valve positions were reversed for downdraft drying. The #6, #7, and #8 valves were used to adjust the wind speed and roasting temperature. The drying parameters had a significant effect on the crack ratio of the pellets. Based on the thermal stability of the HA binder (Figure 1), updraft drying was performed at 300 °C for 5 min. The first downdraft drying stage was performed at 250 °C for 2 min and the second downdraft drying stage was performed at 450 °C for 3 min. The wind speed was fixed at 1.4 m/s for the entire drying process.

After drying, the preheating, firing, soaking, and cooling procedures were subsequently performed. The fired pellets were soaked for 3 min to further improve their compressive strength. The main chemical compositions of the raw materials and the fired pellets were determined by X-ray fluorescence (XRF, Axios, PANalytical B.V., Almelo, The Netherlands). The phases compositions and microstructures of the fired pellets were analyzed by X-ray diffraction (XRD, D8 Advance, BRUKER, Karlsruhe, Germany) and scanning electron microscopy (SEM, MIRA4-LMH, TESCAN, Brno, Czech Republic) with

energy-dispersive X-ray spectroscopy (EDS, Ultim Max 50, TESCAN, Brno, Czech Republic). Chinese standards GB/T 13242-2017, GB/T 13241-2017, GB/T 13240-2018, and GB/T 34211-2017 were used to evaluate the metallurgical properties of the fired pellets. These metallurgical properties include the reducibility index (RI), reduction degradation index (RDI), reduction swelling index (RSI), and softening and dripping properties. The equations used to calculate RI, RDI, and RSI have been previously published [18].

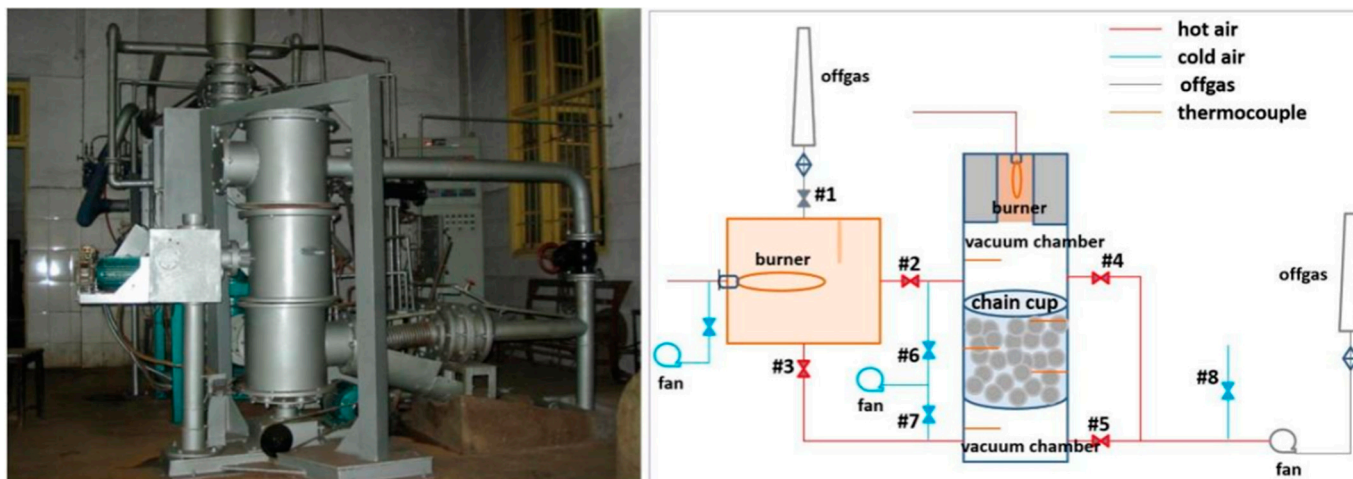


Figure 5. Photograph and schematic diagram of simulated straight-grate facility.

3. Results and Discussion

3.1. Effects of Preheating and Firing Parameters on Fired VTM Pellet Quality

With a fixed wind speed of 2.2 m/s during the preheating and firing processes, the effects of the bentonite and HA binders and the roasting parameters on the qualities of the fired VTM pellets were investigated, and the results are shown in Table 3. Increasing the roasting temperature and roasting time were both conducive to enhancing the qualities of the fired VTM pellets when using 0.75 wt% HA binder. Compared with firing time, firing temperature had a greater effect on the physical properties of the fired VTM pellets. Under a preheating temperature of 950 °C, a preheating time of 18 min, and a firing time of 10 min, the firing temperature was increased from 1280 °C to 1300 °C. With increasing firing temperature, the compressive strength of the fired VTM pellets was enhanced from 1978 N per pellet to 2334 N per pellet and the tumble index (+6.3 mm) increased from 91.0% to 94.2%, while the abrasion index (−0.5 mm) and crack ratio decreased from 6.8% to 3.6% and from 33% to 24%, respectively. As mentioned above, the main phase of the VTM concentrates was titanomagnetite. Increasing roasting temperature and roasting time was therefore conducive to the exsolution of magnetite (Fe_3O_4) and ilmenite (FeTiO_3). This facilitated the oxidation of magnetite and thus improved the compressive and mechanical strength of the fired VTM pellets. Compared to the pellets produced with the bentonite binder, the HA binder pellets required a longer preheating time. This was mainly due to the thermal decomposition temperature of the HA binder, which was between 200 °C and 700 °C (Figure 1).

The fine particles from abrasion then contribute to dust while handling pellets [19]. It is worth noting that dust control has been a major concern for the organic binders explored in recent years. The well-known organic binders CMC and Peridur can be used to produce strong pellets at low dosages, but they typically result in dusty pellets [16]. In contrast, the abrasion index of the fired VTM pellets obtained using the HA binder in this work was controlled to lower than 5%, which conforms to the ISO tumble standard [20]. The improved abrasion resistance was beneficial to minimize fines and dust generation during transport and iron making.

According to the standard for physical properties of second-class fired pellets for blast furnaces (a compressive strength higher than 2300 N per pellet, a tumble index higher than 90%,

and an abrasion index lower than 6%), the recommended oxidation roasting parameters of the HA binder pellets were determined to be: a preheating temperature of 950 °C, a preheating time of 18 min, a firing temperature of 1300 °C, and a firing time of 10 min.

Table 3. Effect of preheating and firing parameters on the qualities of fired VTM pellets using HA binder or bentonite binder.

Binder	Preheating		Firing		Qualities of Fired Pellets			
	T/°C	Time/min	T/°C	Time/min	Compressive Strength/(N/P)	Tumble Index (+6.3 mm)/%	Abrasion Index (−0.5 mm)/%	Crack Ratio/%
HA binder	950	15			1733	88.9	8.9	15
	950	18	1280	10	1978	91.0	6.8	33
	1000	18			2153	93.4	4.5	18
	950	18	1300	10	2344	94.2	3.6	24
			1280	12	2067	91.3	6.9	16
Bentonite	950	15	1280	10	2279	94.1	4.2	10
Standard *	-	-	-	-	≥2300	≥90.0	≤6.0	-

* Standard for physical properties of second-class fired pellets for blast furnace (GB/T 27692-2011).

Typical temperature curves of the simulated straight-grate experiment are shown in Figure 6. As can be seen, the duration from drying to soaking was 45 min, including 10 min of drying, 18 min of preheating, and 10 min of firing. When the roasting temperature was higher than 800 °C, extending the roasting time to 17 min caused the temperatures of the pellets layers to be higher than that of the upper vacuum. This demonstrated that the Fe₃O₄ was oxidized to Fe₂O₃, which was accompanied by a large release of heat. The newly generated Fe₂O₃ atoms were extremely reactive, diffusing within the lattice and migrating to adjacent particles by forming connection bridges, thus increasing the strength of the fired VTM pellets. The upper layer, middle layer, and bottom layer showed the same tendencies with respect to the temperature variation, indicating that the qualities of fired pellets in different layers were homogeneous and stable.

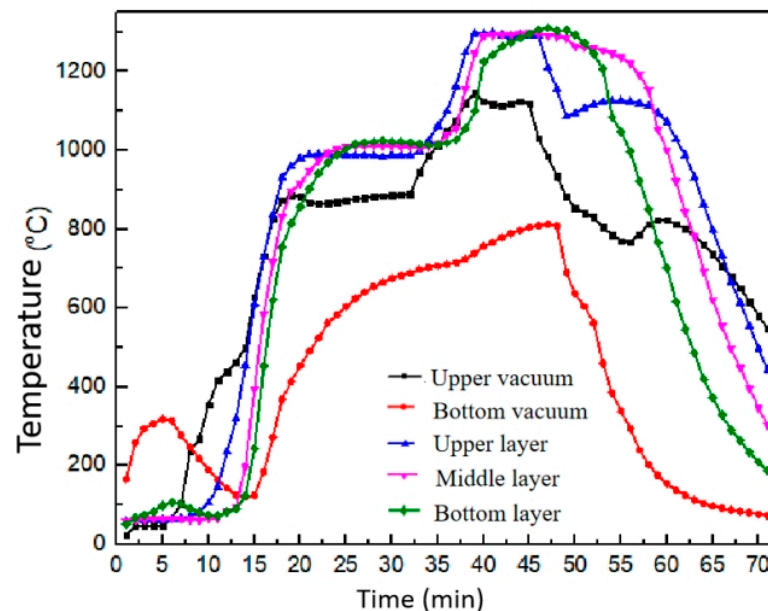
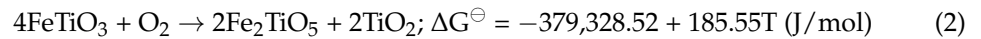
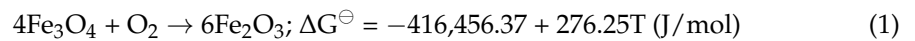


Figure 6. Typical temperature curves of the simulated straight-grate experiment using HA binder.

3.2. Microstructure and Phase Analysis

The phase composition of the fired VTM concentrate pellets obtained using the HA binder, preheating at 950 °C for 18 min and firing at 1300 °C for 10 min, is shown in Figure 7a. The fired pellets mainly consisted of hematite (Fe₂O₃), pseudobrookite (Fe₂TiO₅), and spinel, similar to the phase composition of the bentonite pellets. The formation of

hematite (Fe_2O_3) was due to the oxidation of magnetite (Fe_3O_4) (Equation (1)), while the generation of pseudobrookite (Fe_2TiO_5) was caused by the oxidation of ilmenite (FeTiO_3) (Equation (2)):



SEM-EDS results further demonstrated this process, as shown in Figure 7b–g. The bright white area in the SEM image in Figure 7b represents hematite, while the light grey area is pseudobrookite and the dark grey area is spinel and olivine phases. Figure 7c shows that the Fe_2O_3 crystals are tightly interconnected, beneficial for enhancing the compressive strength of the fired pellets. When Fe_2O_3 crystals coexisted with Fe_2TiO_5 crystals in the VTM pellets, the Fe_2O_3 crystallization growth was inhibited. Therefore, increasing the preheating time was necessary to strengthen Fe_2O_3 crystallization in the VTM pellets during the oxidation process. The spinel phase mainly consists of magnesium, aluminum, and iron, as shown in Figure 7g, and embedded Fe_2TiO_5 particles in the shape of stria. The formation of olivine was mainly due to the existence of magnesium, silicate and ferrous oxides, as shown in Figure 7f. Due to the low content, the diffraction peaks of olivine were hard to observe in Figure 7a. Holes were formed around the well-crystallized olivine, caused by the shrinking liquid phases during the cooling process. These holes are unfavorable for improving the compressive strength of the fired pellets.

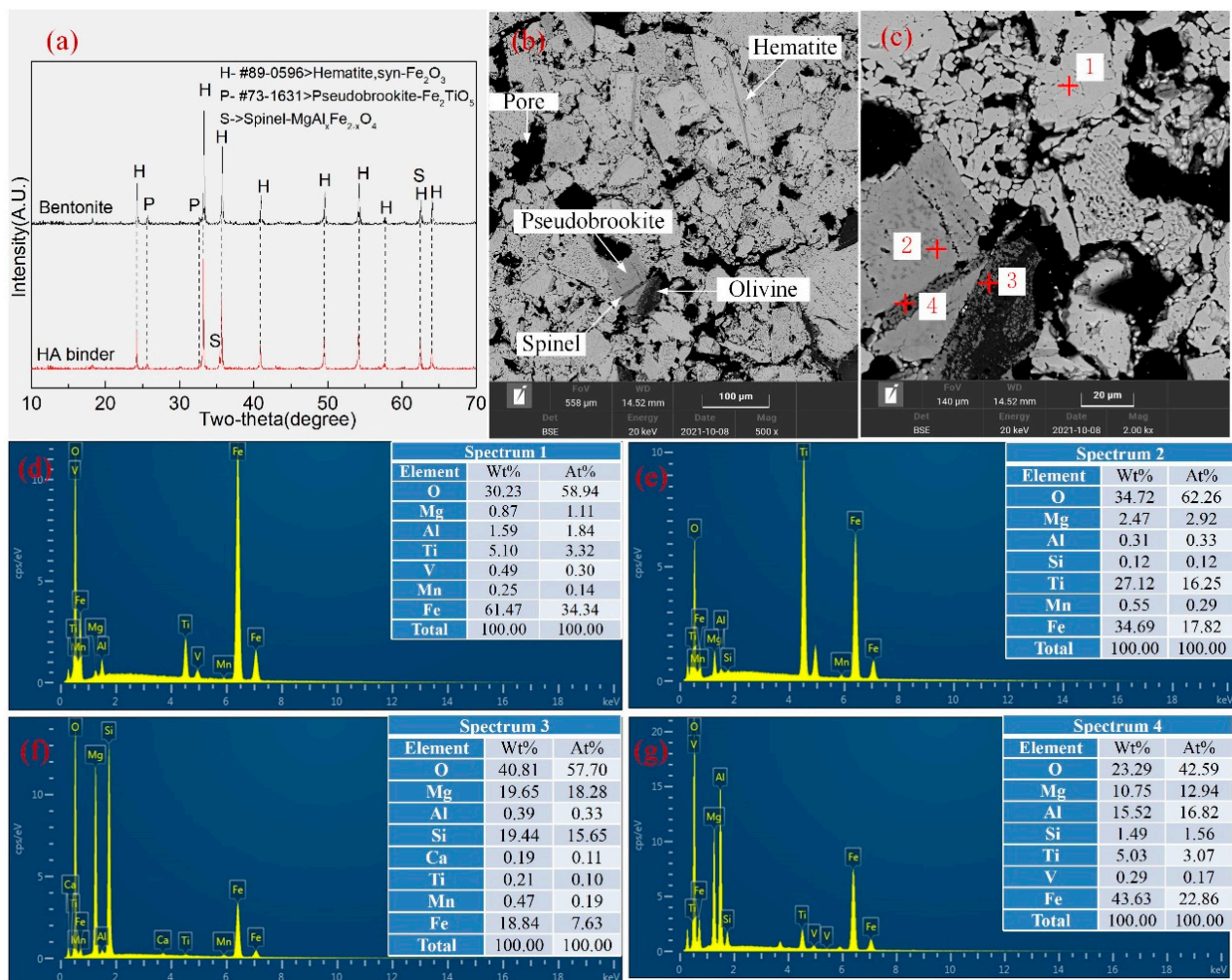


Figure 7. (a) XRD patterns of fired VTM pellets obtained using HA and bentonite binders. (b–g) SEM-EDS analysis of fired VTM pellets obtained using HA binder.

3.3. Metallurgical Properties

A comparison of the chemical compositions of the fired VTM pellets obtained using the bentonite and HA binders are shown in Table 4. It is worth noting that the total iron content of the fired pellets obtained using HA binder was 0.97% higher than that of the pellets obtained using bentonite. Previous investigations have indicated that during blast furnace operation, a 1% increase in the iron grade of fired pellets can reduce the coke ratio by 2% and increase the output of the blast furnace by 3% [20]. Furthermore, the replacement of bentonite with the HA binder could potentially lead to significant economic benefits for blast furnace production. Moreover, the SiO₂ and Al₂O₃ content values of the fired pellets obtained using HA binder were 4.02% and 2.91%, respectively, both lower than the corresponding values of the bentonite pellets. This was mainly due to the low amount of HA binder residues during the roasting process. The FeO content of the HA binder pellets was 0.52% lower than that of the bentonite pellets, conducive to a lower coke ratio in the blast furnace.

Table 4. Chemical composition of the fired VTM pellets obtained using different binders/wt%.

Binder	TFe	FeO	SiO ₂	Al ₂ O ₃	CaO	MgO	TiO ₂	V ₂ O ₅	K ₂ O	Na ₂ O	P	S
Bentonite	53.61	2.09	4.61	3.09	0.75	3.03	11.05	0.59	0.02	0.16	0.01	0.01
HA binder	54.58	1.57	4.02	2.91	0.66	2.97	11.14	0.60	0.02	0.19	0.01	0.01

As an important part of blast furnace operation, pellets with good metallurgical properties are essential for obtaining smooth and successful smelting. The effects of the HA binder and bentonite on the metallurgical properties of the fired VTM pellets were investigated, and the results are presented in Table 5.

Table 5. Metallurgical properties of fired VTM pellets obtained using different binders.

Binder	RI/%	RDI _{+3.15mm} /%	RSI/%	T ₁₀ /°C	T ₄₀ /°C	ΔT ₁ /°C	T _d /°C	ΔT ₂ /°C
Bentonite	59.59	97.98	10.56	1051	1182	131	1299	248
HA binder	58.40	98.71	9.35	1075	1184	109	1285	210

T₁₀: softening start temperature; T₄₀: softening finishing temperature; T_d: dripping temperature; ΔT₁: softening interval; ΔT₂: soft melting interval.

The reducibility index (RI) has a significant effect on the production and energy efficiency of a blast furnace. As shown in Table 5, the reducibility index of the fired pellets obtained using the HA binder was 58.40%, slightly lower than the RI of the bentonite pellets. The reduction disintegration index (RDI_{+3.15mm}) is closely related to the gas permeability and productivity of the blast furnace. The RDI_{+3.15mm} value of the HA binder pellets was 98.71%, indicating favorable gas permeability in blast furnaces. Another important factor is the reduction swelling index (RSI), which should be below 20% for smooth blast furnace operation. Table 5 shows that the RSI values of the HA binder pellets and bentonite pellets were 9.35% and 10.56%, respectively, both satisfying the requirements of blast furnace operation.

The softening start temperature (T₁₀) of the HA binder pellets was 24 °C higher than that of the bentonite pellets. In contrast, the softening finish temperature (T₄₀) of the HA binder pellets was similar to that of the bentonite pellets. Thus, the softening interval (ΔT₁) of the HA binder pellets was narrower than that of the bentonite pellets, conducive to gas permeability and smooth blast furnace operation. The dripping temperature of the HA binder pellets was 14 °C lower than that of the bentonite pellets. Narrower softening melting intervals are more favorable for blast furnace operation. Therefore, compared to the bentonite pellets, the addition of the HA binder both improves the iron grade of the fired pellets and promotes their metallurgical properties.

4. Conclusions

With the rapid development of iron ore pellets, the exploitation of a new composite binder to effectively improve the quality and reduce the production cost of pellets is highly

desirable. HA binder was extracted from abundant low-cost lignite reserves to realize the natural combination of organic and inorganic functional components. A pilot-scale straight-grate experiment used for the oxidation roasting of vanadium–titanium magnetite concentrates showed that the replacement of a bentonite binder with HA binder was feasible. Using 0.75 wt% HA binder instead of 1.5 wt% bentonite binder resulted in fired VTM pellets with better metallurgical properties and 0.97% higher total iron content. This could therefore be beneficial in reducing the ironmaking cost and improving the output and quality of pellet production at the same time. The main phase composition of the fired VTM pellets obtained using the HA binder included hematite, pseudobrookite, spine and olivine phases, similar to the bentonite pellets. Under a preheating temperature of 950 °C, a preheating time of 18 min, a firing temperature of 1300 °C, and a firing time of 10 min, the compressive strength of the fired HA binder pellets reached up to 2344 N per pellet, higher than that obtained with the bentonite pellets. The findings can not only provide a guide for developing a new route for VTM oxidized pellet production, but also be very useful for the application of HA binder in pelletizing production of magnetite concentrate, hematite concentrate, etc.

Author Contributions: Writing—original draft preparation, Y.Y.; writing—review and editing, X.Z.; experimental guidance, X.Z. and G.L.; sample preparation and data analysis, P.C., Y.Z., J.Z. and J.H.; responsible for the whole experiment, P.C., Y.Z., J.Z. and Y.Y.; funding acquisition X.Z. and G.L. All authors have read and agreed to the published version of the manuscript.

Funding: This work was supported by the National Key Research and Development Program of China (No. 2020YFC1909800) and China Postdoctoral Science Foundation (No. 2021TQ0370).

Institutional Review Board Statement: Not applicable.

Informed Consent Statement: Not applicable.

Data Availability Statement: The data presented in this study are available within the manuscript.

Conflicts of Interest: The authors declare no conflict of interest.

References

1. Kawatra, S.K.; Claremboux, V. Iron Ore Pelletization: Part I. Fundamentals. *Miner. Process. Extr. Metall. Rev.* **2021**, 1–16. [[CrossRef](#)]
2. Halt, J.A.; Roache, S.C.; Kawatra, S.K. Cold Bonding of Iron Ore Concentrate Pellets. *Miner. Process. Extr. Metall. Rev.* **2015**, *36*, 192–197. [[CrossRef](#)]
3. Lu, J.; Zhao, X.; Yuan, Z.; Gao, P.; Li, L. Characterization of the Bonding Effect of Nano-CaCO₃ Modified CMC on Magnetite Concentrate Pellets. *JOM* **2019**, *71*, 2549–2555. [[CrossRef](#)]
4. Kawatra, S.K.; Claremboux, V. Iron Ore Pelletization: Part II. Inorganic Binders. *Miner. Process. Extr. Metall. Rev.* **2021**, 1–20. [[CrossRef](#)]
5. Mohamed, O.A.; Shalabi, M.E.H.; El-Hussiny, N.A.; Khedr, M.H.; Mostafa, F. The role of normal and activated bentonite on the pelletization of barite iron ore concentrate and the quality of pellets. *Powder Technol.* **2003**, *130*, 277–282. [[CrossRef](#)]
6. Wang, C.; Xu, C.; Liu, Z.; Wang, Y.; Wang, R.; Ma, L. Effect of organic binders on the activation and properties of indurated magnetite pellets. *Int. J. Miner. Metall. Mater.* **2021**, *28*, 1145–1152. [[CrossRef](#)]
7. Halt, J.A.; Kawatra, S.K. Review of organic binders for iron ore concentrate agglomeration. *Min. Metall. Explor.* **2014**, *31*, 73–94. [[CrossRef](#)]
8. Lu, S.; Yuan, Z.; Zhang, C. Binding mechanisms of polysaccharides adsorbing onto magnetite concentrate surface. *Powder Technol.* **2018**, *340*, 17–25. [[CrossRef](#)]
9. De Moraes, S.L.; Lima, J.R.B.D.; Neto, J.B.F.; Fredericci, C.; Saccoccio, E.M. Binding Mechanism in Green Iron Ore Pellets with an Organic Binder. *Miner. Process. Extr. Metall. Rev.* **2020**, *41*, 247–254. [[CrossRef](#)]
10. Qiu, G.; Jiang, T.; Fa, K.; Zhu, D.; Wang, D. Interfacial characterizations of iron ore concentrates affected by binders. *Powder Technol.* **2004**, *139*, 1–6. [[CrossRef](#)]
11. Zhou, Y.; Kawatra, S.K. Humic Substance-based Binder in Iron Ore Pelletization: A Review. *Miner. Process. Extr. Metall. Rev.* **2017**, *38*, 321–337. [[CrossRef](#)]
12. Copeland, C.R.; Claremboux, V.; Kawatra, S.K. A Comparison of Pellet Quality from Straight-grate and Grate-kiln Furnaces. *Miner. Process. Extr. Metall. Rev.* **2019**, *40*, 218–223. [[CrossRef](#)]
13. Athayde, M.; Cotta, L.C.V.S.; Bagatini, M.C. Case Study of Thermal Profile Design for Traveling Grate Pellet Furnace. *Miner. Process. Extr. Metall. Rev.* **2019**, *40*, 24–34. [[CrossRef](#)]

14. Chen, W.; Dong, Z.; Jiao, Y.; Liu, L.; Wang, X. Preparation, Sintering Behavior and Consolidation Mechanism of Vanadium-Titanium Magnetite Pellets. *Crystals* **2021**, *11*, 188. [[CrossRef](#)]
15. Han, Y.; Kim, S.; Go, B.; Lee, S.; Park, S.; Jeon, H.S. Optimized magnetic separation for efficient recovery of V and Ti enriched concentrates from vanadium-titanium magnetite ore: Effect of grinding and magnetic intensity. *Powder Technol.* **2021**, *391*, 282–291. [[CrossRef](#)]
16. Eisele, T.C.; Kawatra, S.K. A review of binders in iron ore pelletization. *Miner. Process. Extr. Metall. Rev.* **2003**, *24*, 1–90. [[CrossRef](#)]
17. Zhang, Y.; Lu, M.; Zhou, Y.; Su, Z.; Liu, B.; Li, G.; Jiang, T. Interfacial Interaction between Humic Acid and Vanadium, Titanium-Bearing Magnetite (VTM) Particles. *Miner. Process. Extr. Metall. Rev.* **2020**, *41*, 75–84. [[CrossRef](#)]
18. Wang, S.; Guo, Y.; Zheng, F.; Chen, F.; Yang, L. Improvement of roasting and metallurgical properties of fluorine-bearing iron concentrate pellets. *Powder Technol.* **2020**, *376*, 126–135. [[CrossRef](#)]
19. Halt, J.A.; Nitz, M.C.; Kawatra, S.K.; Dubé, M. Iron Ore Pellet Dustiness Part I: Factors Affecting Dust Generation. *Miner. Process. Extr. Metall. Rev.* **2015**, *36*, 258–266. [[CrossRef](#)]
20. Geerdes, M.; Toxopeus, H.; van der Vliet, C. Ch. 3: The Ore Burden: Sinter, Pellets, Lump ore. In *Modern Blast Furnace Ironmaking: An Introduction*, 2nd ed.; IOS Press: Amsterdam, The Netherlands, 2009; pp. 19–35.